

## **3-D converted-wave seismic processing**

Peter W. Cary<sup>1</sup>

### **ABSTRACT**

A processing flow for 3-D converted-wave (P-S1 and P-S2) seismic data is described.

### **INTRODUCTION**

A 3-D seismic survey acquired with a conventional P-wave source and three-component geophones yields three seismic data volumes (P-P, P-S1 and P-S2). The processing required for the P-P data volume requires no discussion here. Figure 1 outlines the basic steps in processing the P-S1 and P-S2 data volumes to DMO migrated stack. The steps in the converted-wave flow that differ substantially from the P-wave flow will be explained.

The object of the processing of all three data volumes is the same: to produce broad-band, zero-phase, DMO migrated stacks. The amplitudes of all three sections are obtained by averaging the amplitudes of the unmuted portions of the prestack traces. The fact that amplitudes on final sections do not represent zero-offset amplitudes is usually ignored for P-P data (e.g. when interpreting P-P seismic sections with zero-offset synthetic seismograms), but this fact is inescapable with converted-waves since the amplitudes of P-S converted-waves at zero offset over flat reflectors is zero.

Polarity and bin size are important issues in the acquisition, processing and interpretation of three-component data. I believe that the final results of converted-wave processing should be three volumes that are as easy as possible for the interpreter to interpret. This implies that the final three volumes should have the same bin size (equal to the P-P bin size) and that the three volumes should correlate with each other without polarity reversals.

### **THE 3-D FLOW**

#### **P-P processing**

The first step is to process the 3-D P-P volume at least to the brute stack stage, and preferably to final migrated stack. This should be done before processing the converted-wave volumes since the P-wave shot statics, the P-wave structure statics and the P-wave stacking velocities are needed for the P-S data processing.

---

<sup>1</sup>Pulsonic Geophysical Ltd.

## Geometry assignment and polarity correction

The orientation of the 3-component geophone axes and the result of geophone tap tests are required for proper 3-D converted-wave processing. Two azimuth measurements are required for each trace: one for the azimuth of the shot-to-receiver vector (measured positive clockwise from grid North) and one for the azimuth of the H1 axis (measured positive clockwise from grid North). The polarities of the P-P, P-H1 and P-H2 components also need to be modified (if required) to conform to the recommendations of the SEG standards subcommittee on multicomponent data (Pruett, 1987), which is supported by the CREWES Project (Stewart and Lawton, 1994). Once the data are processed according to this convention, the P-P, P-S1 and P-S2 volumes can be correlated with each other, with a positive peak on the final sections representing a reflection from a zone of increasing impedance. If a geophone conforms to the SEG recommendation, then the results of the tap tests should be the same as those described in Figure 2. Reflections from a positive impedance contrast should cause negative numbers to be recorded on tape on all three components. The polarities of all three components therefore need to be reversed in processing once it has been determined that the geophone polarities conform to the SEG recommendation. The polarities of synthetic seismograms and VSP's that are used to interpret the three-component surface-seismic data also need to conform with this polarity standard.

## Birefringence analysis

Shear-wave splitting (birefringence) due to azimuthal anisotropy is commonly observed with converted-wave data. Mode-converted reflections from shallow horizons often observed on the transverse component of 2-D converted-wave data, which implies that shear-wave splitting occurs in near-surface layers. Changes in polarization direction have also been observed to vary with depth (e.g. Winterstein and Meadows, 1991) and also with position along a seismic line (e.g. Ata et al., 1994). At this early stage in the history of converted-wave exploration it is considered sufficient to assume that there is one "natural" coordinate system for the entire dataset that defines the S1 (fast) and S2 (slow) shear-wave polarization directions. Figure 3 shows the geometry of the S1 and S2 coordinate system with respect to the acquisition coordinates, H1 and H2. Alford rotation (Alford, 1986) is normally used to determine the azimuth of the S1, S2 coordinate system for shear-wave source data. Alford rotation cannot be used with converted-wave data. For converted-wave data, the method based on radial-to-transverse energy ratios (Garotta and Granger, 1988) and the method based on cross-correlation modeling (Harrison, 1992) can be used. Both of these methods can be applied on either prestack or poststack data, however it requires considerably less effort to apply them to the prestack data. If stacking is performed before birefringence analysis, great care must be taken to apply exactly the same scaling, statics, and deconvolution operators to each pair of (P-H1 and P-H2) traces. Harrison's method was developed for 2-D converted-wave data, but it is easily extended to 3-D. The algorithm involves doing a least-squares best fit of the crosscorrelation of each pair of rotated and delayed P-H1 and P-H2 traces with a "synthetic" crosscorrelation function, which is estimated from the P-H1 and P-H2 autocorrelation function. The results of the analysis of each trace are averaged with those of all other traces in order to determine the most likely rotation angle and time delay.

## Rotation into natural coordinates and polarity reversals

After determining the correct rotation angle, it is a simple matter to rotate the horizontal components from (P-H1, P-H2) coordinates into (P-S1, P-S2) coordinates. After rotation it is necessary to reverse the polarity of the traces on the "trailing half-

plane" of the spread (the 3-D version of reversing the polarity of the trailing half of a split-spread on a 2-D line) in order to prevent opposite polarity traces from stacking against each other within common-conversion-point (CCP) gathers. The polarity of the P-S1 traces with source-to-receiver vectors that project onto the negative S1 axis need to be reversed, and the polarity of the P-S2 traces with source-to-receiver vectors that project onto the negative S2 axis need to be reversed.

### **Geometrical spreading correction and trace edits**

Ursin (1990) and Harrison (1992) have shown how an appropriate geometrical spreading correction can be applied that is based on P-S stacking velocities. However, since these velocities are not normally known until later in the flow, it is standard to use some offset-independent function to all traces, or else an offset-dependent function that is determined by a statistical analysis of rms amplitudes. Editing of bad traces, bad shots and bad receivers is done at this point, rather than before rotation, since rotation requires all pairs of horizontal-component traces to exist.

### **Amplitudes and deconvolution**

It is desirable to do both residual amplitude compensation and deconvolution in a surface-consistent manner in order to preserve amplitude-versus-offset behaviour. In practice, surface consistent amplitude balance is often replaced by trace-by-trace amplitude balance. The slight loss of accuracy that may occur by not balancing amplitudes in a surface-consistent manner is compensated by the increased accuracy obtained by suppressing the amplitude of noisy traces. If surface-consistent amplitude recovery is desired, then great care must be taken to ensure that individual high-amplitude traces are not corrupting the surface-consistent analysis.

The combination of surface-consistent deconvolution and zero-phase (whitening) deconvolution normally gives a wavelet on final sections with a consistent phase spectrum and a broadband amplitude spectrum (Cary and Lorentz, 1993). In order to keep wavelets as consistent as possible between the horizontal components it is best to design the deconvolution operators with a surface-consistent decomposition of one component, P-S1, and apply those operators to both the P-S1 and P-S2 components. The same type of procedure can be performed with surface-consistent amplitude balancing as well, i.e. the amplitude corrections can be determined by analysing the P-S1 component and applied to the P-S1 and P-S2 components.

### **Initial shear-wave (receiver) statics**

After applying P-wave source statics, brute converted-wave velocities (which can be estimated in a simple manner from the P-P stacking velocities by assuming constant  $V_p/V_s$ ), and an initial mute, the large shear-wave receiver statics can be obtained from common-receiver stacks using the method of Cary and Eaton (1993). Before forming the common-receiver stacks, the converted-wave (CCP) structure statics should be removed as well as possible. The converted-wave structure can be estimated by measuring the P-P structure static on the P-P stack, and converting to P-S structure with a constant  $V_p/V_s$ . Three of the four terms that determine the static on a converted-wave trace (source, offset and structure) can thereby be effectively removed, so the large shear-wave statics can be determined without fear of corrupting geologic structure. This method cannot be expected to work well in complex geologic areas. For most 3-D surveys, the common-receiver stacks are high fold, which can help considerably in determining shear-wave statics.

## **Asymptotic CCP stack**

At this point an initial asymptotic CCP stack can be formed with some chosen bin size. As Lawton (1993b) has pointed out, 3-D converted-wave data is most naturally binned with a bin size that is determined by the separation of subsurface reflection points. This separation is given by  $dR/(1+V_s/V_p)$ , where  $dR$  is the receiver interval. For  $V_p/V_s = 2.0$ , this implies a CCP bin size of  $2dR/3$ , whereas the CMP bin size is  $dR/2$ . The design of the 3-D survey will determine at this point how best to bin the data. Since this is only an intermediate product, it is quite likely that using overlapping CMP-size bins will be sufficient. It would simplify processing to use only one bin size at all stages of the processing of all three components, however it may be best in many cases to use the natural CCP bin size for intermediate processing of the horizontal components.

## **Residual statics and velocity analysis**

At this point the processing of the P-S1 and P-S2 datasets should become independent in the sense that any further statics and velocity analysis should be done separately on the two datasets. We expect the two datasets to have different stacking velocities since their separate existence is caused by anisotropic velocities. The independent S1 and S2 velocities in the near-surface layers can be expected to cause different residual static solutions as well. It is likely that the same near-surface layers that cause most of the shear-wave splitting also cause the large, independent P-S1 and P-S2 shear-wave statics, so it may even be necessary to split the flow as early as the point where the initial large receiver statics are estimated.

Note that the asymptotic CCP brute stack that is used for forming the external pilot traces for residual statics will be incorrect in the shallow section since depth-variant binning is required for accurate stacking (Eaton et al., 1990). Therefore it is important to use a deep time window for the crosscorrelation analysis. Notice that a depth-variant stack cannot be used for obtaining more accurate crosscorrelations since depth-variant binning (and partial stacking) destroys the surface consistency of the data.

After residual statics are determined, velocity analysis is performed on asymptotically gathered CCP supergathers (using either the "natural" CCP bin size or the CMP bin size). Slotboom (1990) has derived a "shifted-hyperbola" normal moveout equation for converted-waves that is more accurate than the conventional equation at large offsets. This equation is used for velocity analysis and normal moveout application.

## **Final asymptotic CCP stack, initial depth-variant CCP stack**

At this point the velocities at depth, where asymptotic binning is appropriate, will be fairly accurate, if the signal-to-noise ratio is good. Therefore, a final asymptotic CCP stack can be made. In the shallow section, the velocity analysis has to be performed after either depth-variant binning or P-S dip moveout so that the traces that stack at the same CCP position are analysed. An initial depth-variant CCP stack at this point will probably reveal some deterioration in the shallow section due to mis-stacking.

The algorithm that is used for depth-variant binning is based on the solution of the quartic equation that defines the converted-wave reflection point, as given by Tessmer and Behle (1988). For 3-D data, it is necessary to allow  $V_p$  and  $V_s$  to vary with time and spatial location around the 3-D grid. Since this equation is quite time-

consuming to solve for every trace, effort has been put into the optimization of this binning process. Tables that define the manner in which a trace of a given offset is "broken up" into several traces that stack into different CCP bins are defined at any number of control points around the 3-D grid. After these tables are defined, the exact manner in which an input trace with a given offset and (x,y) location is depth-variantly binned is rapidly determined with bilinear interpolation between the nearest control points. The data can then be either partially stacked into depth-variant CCP gathers, or taken to full depth-variant CCP stack.

### **Zero-phase deconvolution and trim statics**

A certain amount of improvement of the bandwidth of the data can usually be obtained at this point with zero-phase deconvolution and with trim statics on asymptotic CCP gathers. Care must be taken to limit the bandwidth during zero-phase deconvolution so that noise is not amplified excessively. Care with the application of trim statics is also required since it is possible for the trim statics to enhance the stacking of coherent noise, which tends to be more prevalent in converted-wave data than in P-P data.

### **Final velocity analysis on supergathers after P-S dip moveout**

Converted-wave dip moveout (DMO) has at least three effects on the seismic data: (1) it makes stacking velocities independent of dip by removing reflection-point smear, (2) it performs depth-variant binning of reflections to their CCP position, and (3) it filters out coherent noise with impossibly steep dips and improves the signal-to-noise ratio, especially at large offsets. Using DMO as a noise attenuator may be its most important function for many converted-wave datasets because of problems with noise. Picking velocities after converted-wave DMO is worth doing even in areas with very simple geology because of the improved signal-to-noise ratio. DMO can also be effectively used as a "smart" interpolator (Deregowski, 1986) as long as the interpolation distance is small. So for 3-D surveys that are acquired with a wide range of azimuths, 3-D DMO can be used to interpolate the converted-wave data from its natural CCP bin size to the more desirable CMP bin size. Applying converted-wave DMO to narrow-azimuth range 3-D's can also be done, but is likely to force an anisotropic appearance in the signal-to-noise ratio: the data will appear "cleaner" in the source-to-receiver direction than in the crossline direction.

Harrison (1992) has described a Kirchhoff algorithm for applying dip moveout to 2-D converted-wave data in both the constant  $V_p$ ,  $V_s$  case, and for the vertically varying  $V_p(z)$ ,  $V_s(z)$  case. This algorithm is extended to 3-D in a straightforward fashion. For the constant  $V_p$ ,  $V_s$  case, the 3-D converted-wave dip moveout operator reduces to a 2-D operator aligned along the shot-to-receiver direction. This is because the zero-offset raypath perpendicular to the converted-wave prestack migration impulse response intersects the surface along the line between the shot and receiver, just like P-P DMO (Hale, 1988). However, the constant velocity P-S DMO operator is of very limited use because the CCP binning that P-S DMO performs should be done for the variable velocity case. For the case of velocity that increases with depth, raypath bending leads to a 3-D migration to zero offset (MZO) operator (Perkins and French, 1990). The inline component of the MZO operator contains most of the DMO energy, so in practice the constant velocity DMO operator is usually used on P-P data, especially in simpler geologic settings. The 3-D converted-wave DMO operator for variable  $V_p(z)$  and  $V_s(z)$  has been approximated with a 2-D operator along the shot-to-receiver direction. We have implemented the variable-velocity DMO operator with the method suggested by Harrison (1992), i.e. the average P- and S-wave velocities are

used in the constant velocity DMO equations. This method is not exact, but is accurate within a moderate range of geologic dips.

### **Apply final P-S NMO velocities and mutes**

Once final velocities are picked from supergathers after DMO, final mutes can be determined. The offset range where most useful converted-wave energy is recorded is in the mid-offset range (Lawton, 1993a), so the final mute zone is not much different from that used on P-wave data. Experience has shown that it is usually not of much benefit to mute the near-offset range of traces, even though weak converted-wave amplitudes are expected there.

### **Final P-S DMO stack or depth-variant CCP stack**

The final stack before migration can be either with or without converted-wave DMO. Depending on the bin size used for processing, it may be necessary to interpolate to the CMP bin size at this point. A method based on interpolation in the f-xy domain (Spitz, 1990) would be desirable because of its ability to simultaneously preserve dips and attenuate random noise.

### **Migration**

Harrison and Stewart (1993) have shown that P-S diffractions in an inhomogeneous medium are approximately hyperbolic. The resulting migration velocity that best collapse these diffractions is 6 to 11 percent less than the corresponding P-S rms velocities.

## **FUTURE WORK**

Future work on 3-D converted-wave processing will likely focus on areas such as space- and time-variant shear-wave splitting, wavefield separation, multiple attenuation, coherent noise attenuation, prestack migration, and increased resolution. Even without any further advances, however, it is now possible to produce high-quality 3-D converted-wave images that can provide a wealth of new information to the interpreter.

## **REFERENCES**

- Alford, R.M., 1986, Shear data in the presence of azimuthal anisotropy: Dilleys, Texas: 56th Ann. Internat. Mtg., Soc. Expl. Geophys., Expanded Abstracts, 476-479.
- Ata, E., Michelena, R.J., Gonzales, M., Cerquone, H., and Carry, M., 1994, Exploiting P-S converted-waves: Part 2, application to a fractured reservoir: 64th Ann. Internat. Mtg., Soc. Expl. Geophys., Expanded Abstracts, 240-243.
- Cary, P.W. and Eaton, D.W.S., 1992, A simple method for resolving large converted-wave (P-SV) statics: *Geophysics*, **58**, 429-433.
- Cary, P.W. and Lorentz, G.A., 1993, Four-component surface-consistent deconvolution: *Geophysics*, **58**, 383-392.
- Deregowski, S.M., 1986, What is DMO?: *First Break*, **4**, 7-24.
- Eaton, D.W.S., Slotboom, R.T., Stewart, R.R., and Lawton, D.C., 1990, Depth-variant converted-wave stacking: 60th Ann. Internat. Mtg., Soc. Expl. Geophys., Expanded Abstracts, 1107-1110.

- Garotta, R. and Granger, P.Y., 1988, Acquisition and processing of 3C X 3-D data using converted waves: 58th Ann. Internat. Mtg., Soc. Expl. Geophys., Expanded Abstracts, 995-997.
- Hale, I.D., 1988, Dip moveout processing, SEG course notes.
- Harrison, M., 1992, Processing of P-SV surface-seismic data: Anisotropy analysis, dip moveout and migration, Ph.D. thesis, University of Calgary.
- Harrison, M. and Stewart, R.R., 1993, Poststack migration of P-SV seismic data: *Geophysics*, **58**, 1127-1135.
- Lawton, D.C., 1993a, P-SV acquisition design and the concept of the P-SV zero-offset section: 63rd Ann. Internat. Mtg., Soc. Explor. Geophys., Expanded Abstracts, 562-565.
- Lawton, D.C., 1993b, Optimum bin size for converted-wave 3-D asymptotic mapping: CREWES Research Report, vol. 5.
- Perkins, W.T. and French, W.S., 1990: 3-D migration to zero offset for a constant velocity gradient: 60th Ann. Internat. Mtg., Soc. Expl. Geophys., Expanded Abstracts, 1354-1357.
- Pruett, R., 1987, Acquisition, processing, and display conventions for multicomponent seismic data: Soc. Expl. Geophys. Technical Standards Committee Report (Subcommittee on 3-C Orientation).
- Slotboom, R.T., 1990, Converted-wave (P-SV) moveout estimation: 60th Ann. Internat. Mtg., Soc. Expl. Geophys., Expanded Abstracts, 1104-1106.
- Spitz, S., 1990, 3-D Seismic interpolation in the F-XY domain: 60th Ann. Internat. Mtg., Soc. Explor. Geophys., Expanded Abstracts, 1641-1643.
- Stewart, R.R. and Lawton, D.C., 1994, 3C-3D Seismic Polarity Definitions, Notes from CREWES Workshop on 3C-3D Seismic Exploration, Sept. 29, 1994.
- Tessmer, G., and Behle, A., 1988, Common reflection point data-stacking technique for converted waves: *Geophys. Prosp.*, **36**, 671-688.
- Ursin, B., 1990, Offset-dependent geometrical spreading in a layered medium: *Geophysics*, **55**, 492-496.
- Winterstein, D.F., and Meadows, M.A., 1991, Changes in shear-wave polarization azimuth with depth in Cymric and Railroad Gap oil fields: *Geophysics*, **56**, 1349-1364

Process 3-D P-P Volume  
Geometry Assignment and Polarity Correction to SEG Convention  
Birefringence Analysis  
Rotate into Natural Coordinate System (P-H1, P-H2) --> (P-S1, P-S2)  
Polarity Reversal of Traces on Negative Side of (S1,S2) Axes  
Geometrical Spreading Correction  
Trace Edits  
Amplitude Balance  
Surface-Consistent Deconvolution  
Apply Source Statics, Brute Velocities and Initial Mute  
Compute and Apply Receiver-Stack Statics  
Asymptotic Common-Conversion-Point (ACCP) Brute Stack  
Residual Statics using ACCP Pilot  
P-S Velocity Analysis on ACCP Supergathers  
Zero-phase Deconvolution  
Compute and Apply ACCP-Consistent Trim Statics  
Final ACCP Stack, Initial Depth-Variant CCP Stack  
Final P-S Velocity Analysis on Supergathers after P-S DMO  
Apply Final P-S NMO Velocities and Mutes  
Final P-S DMO Stack or Depth-Variant CCP Stack  
Migration

FIG. 1. 3-D converted-wave (P-S1, P-S2) processing flow.

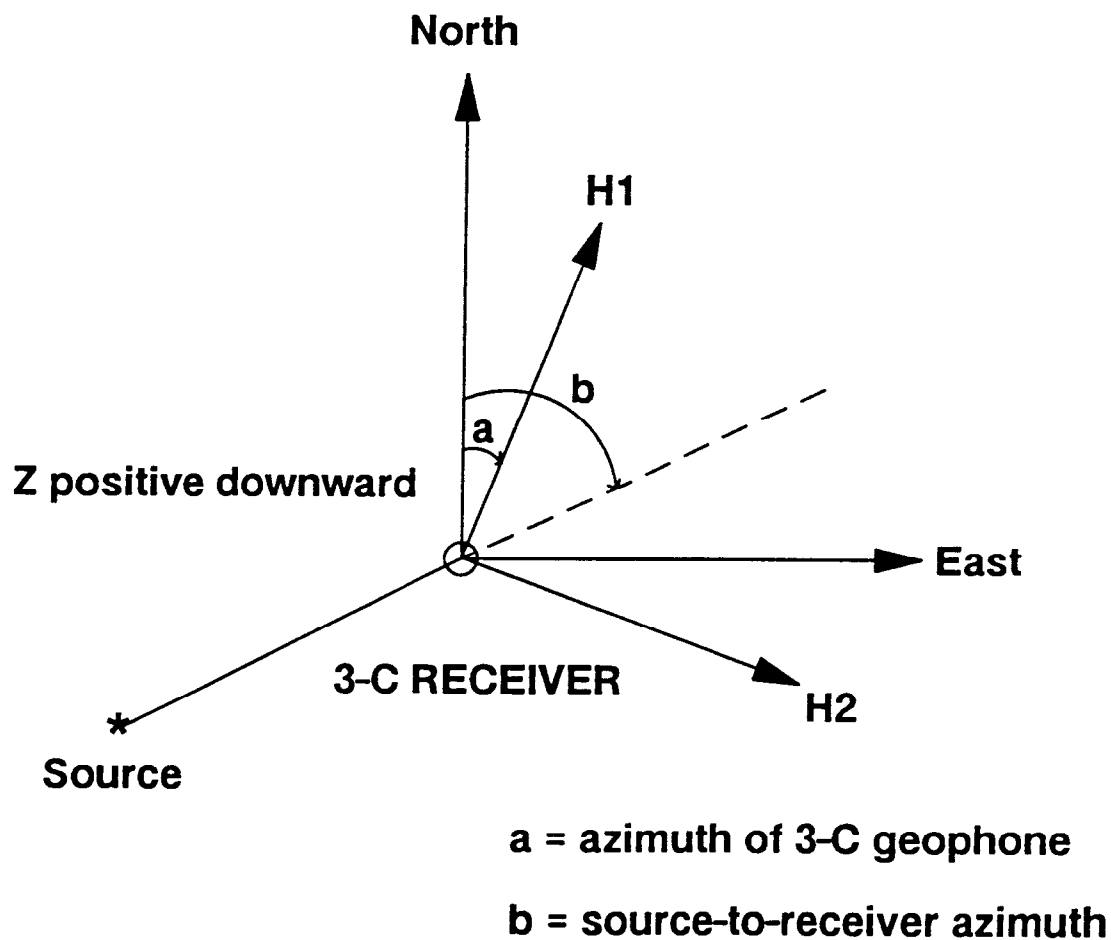


FIG. 2. Plan view (looking down on top of geophone) of 3-C, 3-D geometry. Positive numbers should be recorded on tape when a tap is made on the geophone in the positive direction of each of the H1, H2 and Z axes.

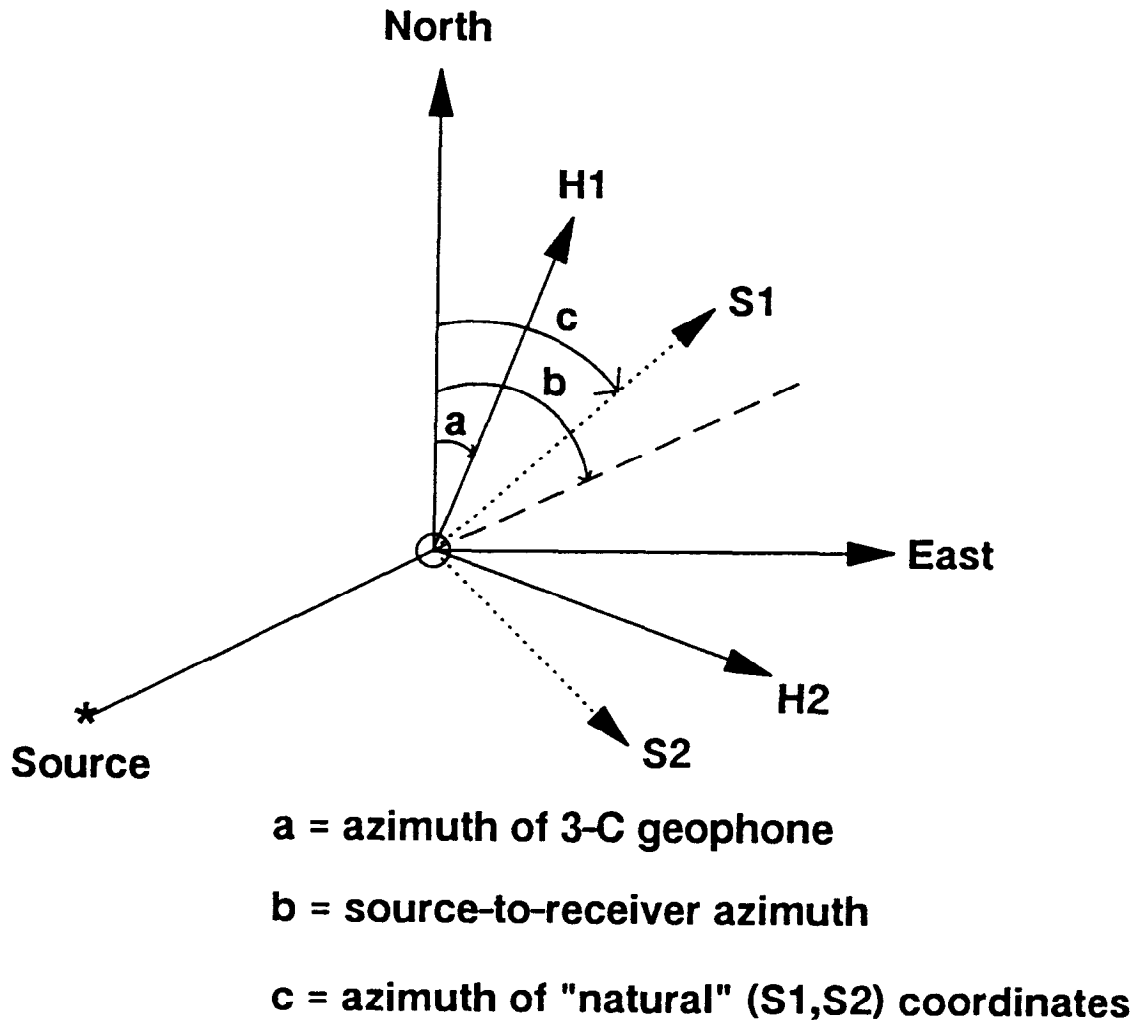


FIG. 3. Converted-wave data require rotation from (H1,H2) acquisition coordinates to the (S1,S2) "natural" coordinates of shear-wave polarization. After rotation, a P-S1 trace with source-to-receiver azimuth,  $b$ , that projects onto the negative S1 axis ( $\cos(b-c) < 0$ ) requires polarity reversal in order for waveforms to stack in-phase within a CCP gather. Similarly, a P-S2 trace with  $\sin(b-c) < 0$  requires polarity reversal.